Nature of Bonding in [3.1.1]Propellane. Vibrational Spectra and Normal Coordinate Analysis of 2,4-Methano-2,4-didehydroadamantane, 2,4-(Dimethylmethano)-2,4-didehydroadamantane, and Their Dihydro Congeners

Lahorija Bistričić

Faculty of Electrical Engineering and Computing, University of Zagreb, Croatia

Goran Baranović,* Dunja Šafar-Cvitaš, and Kata Mlinarić-Majerski*

Rugjer Bošković Institute, P.O.B. 1016, HR-10001 Zagreb, Croatia

Received: August 15, 1996[⊗]

The properties of the propellane bond in 2,4-methano-2,4-didehydroadamantane (**1**) and 2,4-(dimethylmethano)-2,4-didehydroadamantane (**2**) have been determined on the basis of the spectroscopic and chemical evidence. A monitoring of reaction of propellane **2** with dimethyl disulfide by Raman spectroscopy has indicated the cleavage of the central bond between inverted carbon atoms. Raman and infrared spectra of **1** and **2** as well as of their dihydro congeners 2,4-methanoadamantane (**3**) and 2,4-(dimethylmethano)adamantane (**4**) have been recorded. To describe the vibrational and molecular orbital properties of these compounds (harmonic frequencies, heats of formations, bond orders, and charge distributions), AM1 semiempirical calculations were performed. The calculated properties are found to be in fair agreement with the observed ones. By combining the results of spectroscopic investigations and molecular orbital calculations, the central bond between inverted carbon atoms is associated with the highest occupied molecular orbitals in propellanes **1** and **2**. Assuming the transferability of the adamantane scaling factors for force constants within the studied group of molecules, an "*a priori*" assignment of the observed bands has been obtained.

Introduction

Small-ring propellanes are a class of hydrocarbons characterized by three rings joined by a common pair of bridgehead carbon atoms. The features of these highly strained molecules are of particular interest due to the unusual properties of the bond formed by inverted carbon atoms and a variety of interesting reactions.[1] They have therefore been the subject of numerous theoretical investigations,[2−6] X-ray and electron-diffraction analyses,[7] and vibrational[8] and photoelectron[9] spectroscopic studies.

In the analysis of the properties of the bond between inverted carbon atoms apparently opposite conclusions have been reached. The evidence for the existence of the central C−C bond is deduced, as for any other bond, from the electron density contour maps in the interbridgehead regions from molecular orbital calculations. However, according to *ab initio* molecular orbital studies on [1.1.1]propellane, there is no evidence for a central bond in terms of the charge distribution.[2a] The central bond in [1.1.1]propellane is formed from sp^4 hybrid orbitals directed away from each other and with zero overlap population. Feller and Davidson[4] came to the conclusion that [1.1.1]-propellane is just a strained cage with negligible bridgehead to bridgehead through-space covalent bonding. Wiberg et al.[3b] came to a different conclusion assuming that the electronic charge density is a physical property of the system and is model independent. These authors concluded, according to an analysis of the second derivative of the electron density determined by all occupied orbitals, that the bridgehead atoms are bonded to one another because there is an appreciable accumulation of charge between the bridgehead atoms. The results of quasi *ab initio* PRDDO calculations reinforce the conclusion that bridgehead atoms in [1.1.1]propellane are weakly bonded in the ground state.[6b]

Several studies have reported on the strain energy in the small-ring propellanes.[3,5,6a] The bridgehead carbons in the propellanes withdraw charge from neighboring groups to the bridgehead region with increasing strain in these molecules.[3c] A photoelectron (PE) spectroscopic study of [1.1.1]propellane[9a] revealed that there should be only minute changes in geometry between [1.1.1]propellane and its radical cation. This was attributed to the nonbonding or slightly antibonding character of the highest occupied molecular orbital (HOMO) of [1.1.1]-propellane. PE investigation on a less strained [3.1.1]propellane (**1**)[9b] was indicative of a slightly bonding HOMO, while the PE spectra of several [*n*.1.1]propellanes[9c] showed that the energy of the first band depends very strongly on *n*.

From aspects of structure determination and molecular spectroscopy, data on [3.1.1]propellanes are to our knowledge rather scarce. The structure of the substituted aza[3.1.1]-propellane[7d] is known, but it is not very suitable for comparison if, for example, the geometrical parameters are considered. This is, however, one of the few papers dealing with the measured electron charge density. It gives no evidence for the excess charge between the bridgehead carbons. The difference of the electron density of the two [1.1.1]propellane derivatives turned out to be slightly negative between the bridgehead atoms and diffuse and positive outside the bridgehead bond.[7f] The unsubstituted [3.1.1]propellane has not been spectroscopically characerized yet. Therefore, only the [1.1.1]propellane is left for comparison since it has been thoroughly studied by various theoretical and experimental methods. The assignment of vibrational spectra of [1.1.1]propellane was based on *ab initio* MO theory (at the SCF level with the use of the 6-31 G* basis set). The authors reported a stretching force constant 6.2 aJ $Å^{-2}$ for the central C−C bond as evidence of bonding. Reported distances between inverted atoms lie in the range 1.550−1.587 Å, slightly longer than the normal C−C single bond distance of about 1.540 Å.[7,8]

[⊗] Abstract published in *Advance ACS Abstracts,* January 1, 1997.

S1089-5639(96)02503-0 CCC: $14.00

Contrary to the usual carbon−carbon single bond, the central bond in small-ring propellanes, such as in 2,4-methano-2,4-didehydroadamantane (**1**) and 2,4-(dimethylmethano)-2,4-didehydroadamantane (**2**) (Figure 1), is highly reactive toward electrophiles and free radicals.[10−13] The bond in **1** and **2** can easily be reduced by electron-transfer hydrogenation to give 2,4-methanoadamantane (**3**) and 2,4-(dimethylmethano)adamantane (**4**), respectively.[11,12] Also, [3.1.1]propellanes **1** and **2** readily add disulfides and carbon tetrachloride across the central bond to give the corresponding 2,4-disubstituted 2,4-methanoadamantanes.[10] The unusual chemical reactivities of **1** and **2** have been attributed to the electron-density distribution in the central propellane bond.[11,12] Whereas chemical evidence indicates that the electron density on the central bond of small propellanes is considerably higher at the back side of the inverted carbon atoms than between them, more substantial support of this hypothesis was needed. Therefore, we have undertaken a detailed vibrational study of the two [3.1.1]propellane derivatives, **1** and **2**, and their dihydro congeners, **3** and **4**, and determined the changes in energies, geometrical parameters, and normal modes due to the formation of the propellane bond.

Experimental Section

[3.1.1]Propellanes **1** and **2** as well as their dihydro congeners **3** and **4** were synthesized following the literature procedures.[11,12] The samples of **1** and **2** were prepared in a drybox under nitrogen. For Raman spectroscopy capillary tubes were filled with the neat sample and spectra were recorded immediately after. The propellane **1** for the IR spectra was prepared from C_6D_6 solutions between two KBr discs, and the solvent was evaporated before the spectra recording. For the IR spectra, **2** was put neat between two KBr pellets in a drybox filled with nitrogen and the spectrum recorded immediately after. Since it was practically impossible to prevent propellanes **1** and **2** from reacting with oxygen from the air, the strong carbonyl band due to the reaction products[12b] was always present in the recorded IR spectra. In the case of moleule **2** a series of IR spectra with a time lag of 10 min were recorded with the idea of assigning the bands of **2** by their gradual disappearance. Reaction of **2** with dimethyl disulfide was carried out directly in a capillary tube and monitored by Raman spectroscopy.

The IR spectra were recorded from 3100 to 200 cm^{-1} on a Perkin Elmer 580 B spectrometer. Raman spectra without polarization were recorded on a Dilor Z24 triple monochromator coupled with an IBM AT computer. The 514.5 nm line of a Coherent INNOVA-165 Model argon ion laser was used for excitation. The spectra were taken from 3500 to 100 cm^{-1}. Data were processed with the Dilor software.

Results and Discussion

Observed Spectral Characteristics. Examining the reaction of propellane **2** with oxygen (Figure 2), the changes in band intensities can be observed. The intensity of the characteristic vibration of the carbonyl group at 1720 cm^{-1} gradually increases due to the reaction products.[12b] The CH_2 scissoring vibrations are almost independent of the molecular framework. Due to the presence of CH_2 groups in propellane **2** and in the reaction products, the intensity of the band at 1460 cm^{-1}, assigned as CH_2 scissoring, remains constant. Comparison of IR spectra has clearly shown that all other intense and well-resolved bands gradually decrease in intensity and therefore can be considered as vibrational bands of propellane **2**. For this reason it was safe to take the similarly strong bands in the infrared (IR) spectrum of **1** as really belonging to propellane **1**.

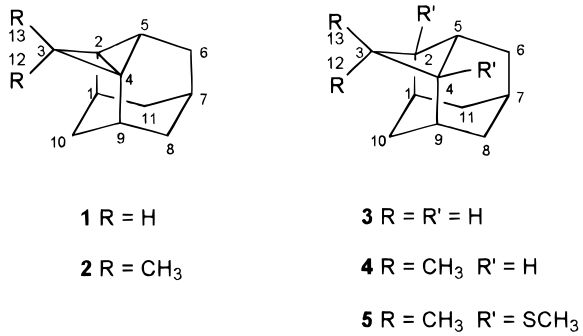

Figure 1. Molecular structure of propellanes **1** and **2**, their dihydro congeners **3** and **4**, and molecule **5** with carbon atom numeration.

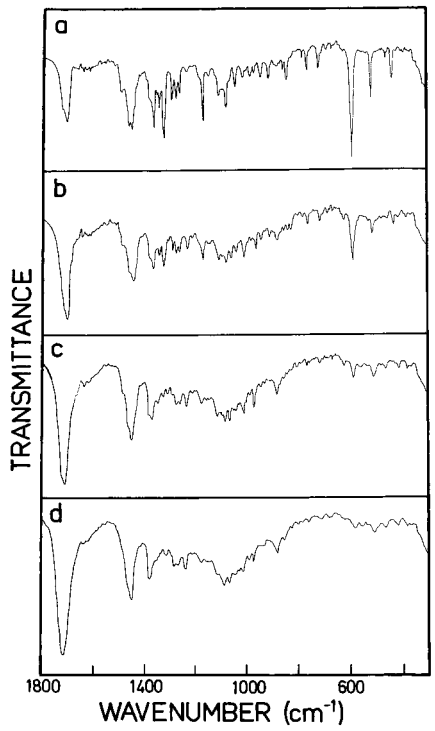

Figure 2. Reaction of **2** with oxygen followed by IR spectroscopy in the 1800−200 cm^{-1} region: (a) 2.5 min, (b) 10 min, (c) 20 min, and (d) 50 min after the reaction started.

If there is a band dominated by the C_2-C_4 stretching, then, by vibrational spectroscopy, it should be possible to monitor the reaction that occurs by the cleavage of the bond between the C_2 and C_4 atoms. Dimethyl disulfide (DMDS) adds spontaneously, at room temperature, across the central bond in propellane **2** to give 2,4-bis(methylthio)-2,4-(dimethylmethano)-adamantane (**5**) as a sole product[12b] (Figure 3). By recording the Raman spectra in the C−C stretching region between 800 and 650 cm^{-1}, the changes in band positions and their relative intensities can be seen (Figure 3). The very intense vibrational band at 764 cm^{-1} disappeared at the end of reaction. Three new signals due to the product **5** appeared at 781, 716, and 679 cm^{-1}. This might be evidence that the band at 764 cm^{-1} is to be associated with the stretching vibration of the bond between inverted atoms (C_2-C_4). The band at 693 cm^{-1} is attributed to the symmetric C−S stretching vibration of DMDS.[14]

As a prerequisite for the interpretation of the spectra recorded during the reaction, we have undertaken an analysis of the Raman (Figures 4−7) and IR spectra (Figure 8) of propellanes **1** and **2** and their dihydro congeners. A very intense IR band occurring at a frequency between 600 and 500 cm^{-1} appears to be characteristic of the small-ring propellanes.[6a,c] According to *ab initio* calculations on [1.1.1]propellane[8a] and MNDO

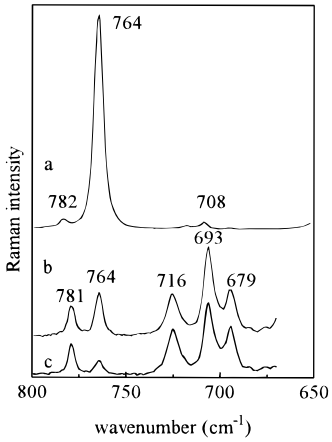

Figure 3. Reaction of **2** with DMDS followed by Raman spectroscopy in the 800−650 cm^{-1} region: (a) spectrum of **2** before the reaction, (b) spectrum recorded immediately after addition of DMDS, and (c) spectrum recorded after 5 min of stirring of the reaction mixture.

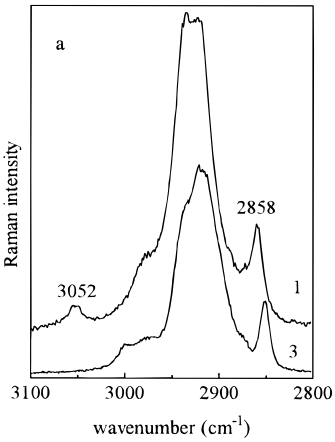

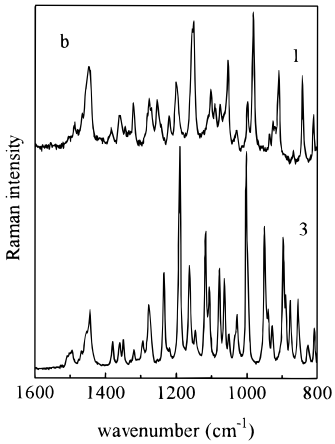

Figure 4. Comparison of Raman spectra of propellane **1** and its dihydro congener **3** in the 3100−800 cm^{-1} region.

calculations[6a] on [1.1.1]- and [2.1.1]propellane, it is assigned to an antisymmetric combination of the peripheral C−C bond stretchings. Its high IR intensity reflects an unusual charge distribution in propellanes, causing the large changes in dipole moment during the vibration. The IR spectra of propellanes **1** and **2** in the region characteristic for propellanes exhibit a very intense band at 580 and 590 cm^{-1}, respectively (Figure 8). There is no such band at that position in IR spectra of their dihydro congeners.

The measured Raman spectra of **1** and **3** differ considerably in the region of the C−C stretching vibrations. The bands at 739 and 672 cm^{-1} in the Raman spectra of **1** might correspond

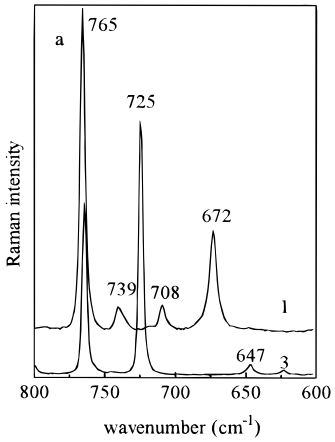

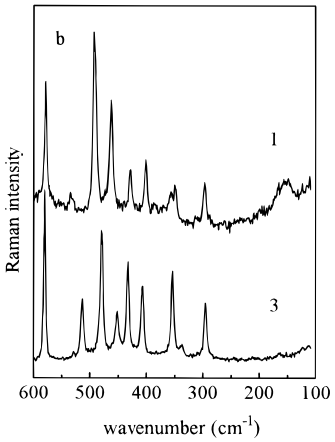

Figure 5. Comparison of Raman spectra of propellane **1** and its dihydro congener **3** in the 800−100 cm^{-1} region.

to the stretching vibration between inverted C_2 and C_4 atoms because those bands were not observed in spectra of **3**. Similar observations can be made for the propellane **2** and its dihydro congener **4**. Experimental evidence from Raman spectra of **2** indicates that the strong Raman band at 764 cm^{-1} and the medium intense band at 840 cm^{-1} should be assigned to the C_2-C_4 stretching motion because they were not found in the spectra of **4**. These Raman bands should correspond to the strong Raman band of [1.1.1]propellane at 908 cm^{-1} assigned to the central C−C bond stretching.[8a] The obtained experimental results seem to provide experimental verification of the existence of a bond between inverted carbon atoms in propellanes **1** and **2**. To gain deeper understanding of the observed spectral characteristics, the fully optimized structure and harmonic force fields of compounds **1**, **2**, **3**, and **4** have been determined by the AM1 calculation method.[15] The calculated force constants were scaled by scaling factors previously optimized for adamantane,[16] and the normal mode frequencies thus obtained were then compared with the observed ones.

Heat of Formation, Bond Orders, and Charge Distribution. To gain insight into the energetics of the molecules **1**, **2**, **3**, and **4**, their heats of formation (ΔH_f) will be discussed (Table 1). The ΔH_f of adamantane is calculated to have a value (−180.79 kJ/mol) that is fairly close to the experimental one (−133.44 kJ/mol).[17] Adamantane has no geometrical strain because all angles are tetrahedral, and it is considerably more stable than **1**, **2**, **3**, and **4**. Unlike adamantane, [1.1.1]propellane is highly strained, and it is not expected that the semiempirical method could predict its properties with comparable accuracy. Relying on the errors in the AM1 heats of formation for adamantane and [1.1.1]propellane, it may be concluded that the heats of formation for **3** and **4** are roughly 2 times more accurate

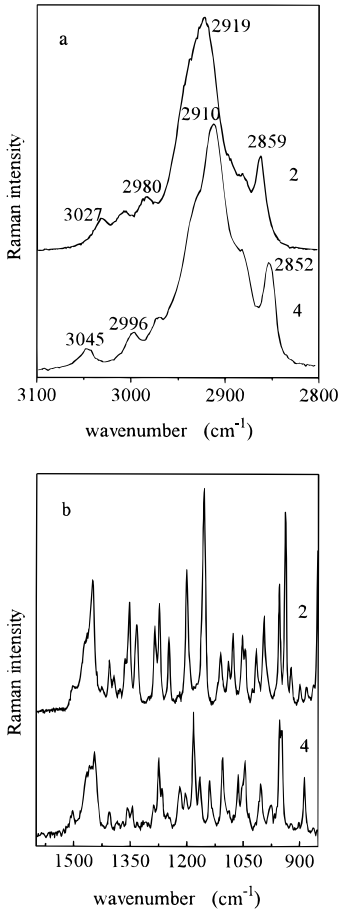

Figure 6. Comparison of Raman spectra of propellane **2** and its dihydro congener **4** in the 3100−850 cm^{-1} region.

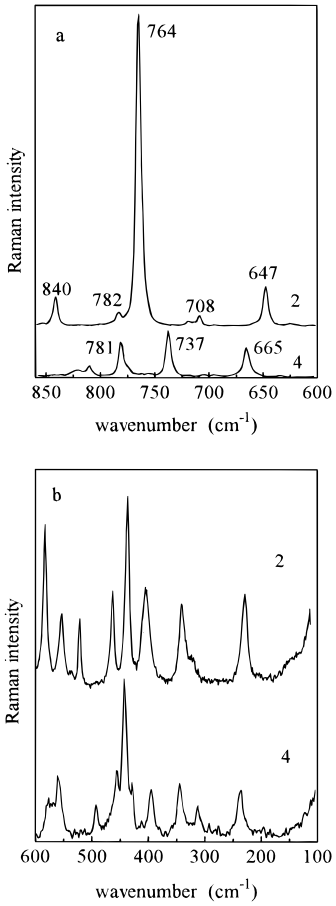

Figure 7. Comparison of Raman spectra of propellane **2** and its dihydro congener **4** in the 850−100 cm^{-1} region.

than for **1** and **2**. The calculated energy of hydrogenolysis (Table 1) of the central bond is −356.1 kJ/mol for **1** and -331.4 kJ/mol for **2** and is explained in terms of the strain energy plus the energy required for the removal of the two hydrogens. The accuracy of these energies may be assessed by comparing the AM1 energy of hydrogenolysis of [1.1.1]propellane (−420.4 kJ/mol) with the value of −192.4 kJ/mol[8a] calculated by taking into account the electron correlation. Its effect on a single-configuration SCF wave function could easily be accounted for in semiempirical calculations as well. However, as is well-known, there is a problem in doing semiempirical CI calculations: the effects of electron correlation are actually counted twice, first in determining parameter values from experimental data and second by introducing configurational interaction itself. Nevertheless, the 3 × 3 CI calculations have been performed and the results for [1.1.1]propellane are in agreement with those obtained by *ab initio* calculations with the 6-31G* basis set.[4] The central bond of the fully optimized ground-state geometry is 0.053 Å longer or, in other words, the CCC angle at the methylene carbons is greater by 2.2° relative to the single-configuration SCF values (the same trend has been confirmed for [3.1.1]propellanes (Tables 1 and 2)). In terms of vibrational frequencies the only significant change is the increase of the A_2'' CCC deformation mode frequency from 577 to 733 cm^{-1}. Since this leads to the ordering of frequencies inconsistent with the experimental one,[8a] the scaling of force constants applied in vibrational assignment of [3.1.1]propellanes has been performed on the force matrices obtained from the single-configuration SCF wave function. A two-configuration SCF wave function includes a configuration corresponding to a HOMO → LUMO double excitation and having a coefficient of −0.28 ([1.1.1]propellane), −0.26 (**1**), and −0.20 (**2**). Thus,

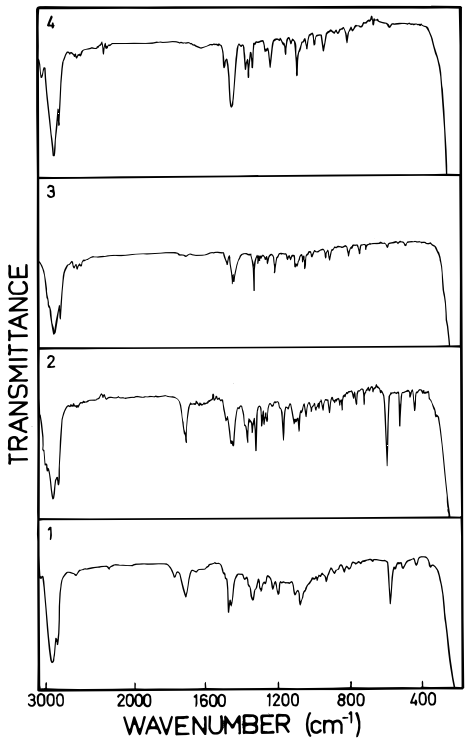

Figure 8. Observed IR absorption spectra (KBr films) of the propellanes **1** and **2** and their dihydro congeners **3** and **4**.

a partial diradical character of the singlet ground state of propellanes is also found in the AM1. In addition, the fully optimized excited diradical singlet state and triplet state of the propellanes have significantly larger energies than the ground

TABLE 1: Heats of Formation and Energies of Hydrogenolysis (kJ/mol) Calculated by AM1

molecule	ΔH_f(exptl) S_0	ΔH_f(calc) S_0	ΔE_{hyd}(calc)	ΔH_f(calc)[d] S_0	ΔH_f(calc)[d] T_1
adamantane	−133.4[a]	−180.0		−175.4	493.0
[1.1.1]propellane	351.4[b]	789.1	−420.4/−192.4[c]	734.7	897.5
1		392.3	−356.1	375.5	458.2
2		375.6	−331.4	364.2	561.4
3		14.5			
4		22.5			

[a] Reference 17. [b] Reference 8a. [c] Reference 8a, the MP3/6-31 G* calculation. [d] Fully optimized ground-state singlet S_0 and first excited triplet T_1 AM1 3 × 3 CI geometries.

TABLE 2: Calculated Equilibrium Values of Some Geometrical Parameters for Propellane 1 and 2 and Their Dihydro Congeners 3 and 4

parameter[a]	**1**	**2**	**3**	**4**
C−H[b]	1.120	1.120	1.120	1.120
C_1-C_2	1.502	1.505	1.536	1.536
C_2-C_3	1.515	1.531	1.561	1.579
$(C-C)_{inv}$ (C_2-C_4)	1.567	1.547	2.130	2.117
	1.712[c]	1.622[c]		
C_2-C_5	1.523	1.526	1.567	1.567
C_5-C_6	1.496	1.496	1.497	1.497
C_6-C_7	1.523	1.523	1.520	1.517
C_7-C_{11}	1.531	1.533	1.529	1.530
C_1-C_{11}	1.529	1.531	1.528	1.532
C_1-C_{10}	1.558	1.558	1.535	1.532
C_3-C_{12}		1.503		1.522
$\angle C_2C_5C_4$	61.9	59.5	85.5	85.0
	68.2[C]	64.2[c]		
$\angle C_2C_3C_4$	62.3	60.7	85.9	84.1
$\angle C_3C_2C_5$	98.2	98.2	86.3	86.7
$\angle C_2C_5C_6$	117.7	118.8	119.2	120.1
$\angle C_3C_2C_1$	122.3	124.8	109.0	111.4
$\angle C_5C_2C_1$	122.3	121.3	110.0	109.1
$\angle C_1C_{10}C_9$	102.5	102.5	106.2	106.1
$\angle C_2C_1C_{10}$	102.6	103.5	109.3	110.9
$\angle C_8C_7C_{11}$	113.0	114.3	113.4	114.8
$\angle C_2C_3C_{12}$		119.1		111.4
$\angle C_{12}C_3C_{13}$		110.0		106.3

[a] Distances C−H and C_i-C_j in angstroms; angles ∠ in degrees. The numbering of atoms is shown in Figure 1. [b] Average value. [c] Two-configuration SCF ground state.

state (Table 1), which might be an indication of bonding in the latter. The increased length of the triplet-state central bond (1.723 Å in [1.1.1]propellane, 1.974 Å in **1**, 1.960 Å in **2**) is consistent with the dependence of the 6-31G* SCF energy of the triplet configuration of [1.1.1]propellane as a function of the central bond length. It may be safely concluded that the overall picture of bonding in [1.1.1]propellane as given by AM1 is consistent with the results of high-level *ab initio* calculations,[4] supporting its use in explaining experimental data on [3.1.1]-propellanes.

Examination of the AM1 molecular orbitals indicates that the central C_2-C_4 bonds in **1** and **2** are associated with the HOMOs (Figure 9). Their orbital energies are −8.97 eV in **1** and −9.00 eV in **2**. The HOMOs of **1** and **2** are σ-type molecular orbitals, and the σ bonds formed between C_2-C_4 bridgehead atoms are pure p hybrids with a bond order of 0.88*e* and 0.89*e* in **1** and **2**, respectively. The other C−C bonds in all molecules are σ bonds of the form 0.4 sp + 0.5 pp with bond orders of 0.97*e*. In contrast to **1** and **2**, the top occupied molecular orbitals of **3** and **4** encompass the entire carbon skeleton with ionization potentials of 10.19 eV (**3**) and 10.07 eV (**4**). Other MOs in all studied compounds are found to be distributed over the entire molecular framework. This is in accordance with the photoelectron spectroscopic investigation of **1** and supported by the MNDO calculations indicating that the HOMO of propellane **1** has a bonding character.[9b]

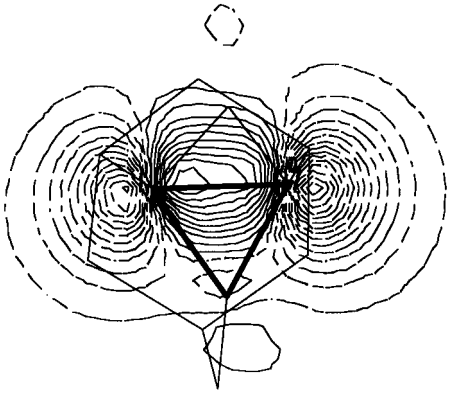

Figure 9. HOMO of **1** showing the electron density along the propellane bond.

To understand better the bonds between the bridgehead C_2 and C_4 atoms, the calculated electronegativity of atoms was also examined. The net charges on the individual C atoms in **1**, **2**, **3**, and **4** are different. The C_2 and C_4 atoms in **3** and **4** bear a charge of −0.11*e* and −0.09*e*, respectively. There is an increase in the electronegativity of C_2 and C_4 atoms on passing from **3** and **4** to propellanes **1** and **2**. The net charges on C_2 and C_4 atoms in **1** are −0.23*e* and −0.22*e* in **2**. The negative charges of carbon atoms C_2 and C_4 increase with increasing strain; they bear the largest negative charge of all the C atoms in **1**, **2**, **3**, and **4**. The C_2 and C_4 atoms in propellanes **1** and **2** withdraw charge from their bonded neighbors (C_1, C_3, C_5, and C_9 atoms according to Figure 1) and they become less electronegative in comparison with the corresponding C atoms in their dihydro counterparts **3** and **4**. The net charges on the carbon atoms in **3** are C_1 (−0.09*e*), C_3 (−0.17*e*), and C_5 (−0.12*e*). The decreasing electron population of these carbons in **1** yield net charges of C_1 (−0.05*e*), C_3 (−0.08*e*), and C_5 (−0.02*e*). A detailed comparison of the net charges for compounds **2** and **4** gave similar results: C_1 (−0.09*e*), C_3 (−0.06*e*), C_5 (−0.125*e*) in **4** and C_1 (−0.04*e*), C_3 (0.036*e*), and C_5 (−0.032*e*) in **2**. The net charges on the remaining C atoms were almost unchanged and the hydrogen atoms have net positive charge in any of the molecules considered. The increase in the electronegativity of the bridgehead carbon atoms is in connection with increased strain of **1** and **2**. This trend of increasing electronegativity with increasing geometric strain is in accordance with results obtained by Wiberg et al.[3c] for [1.1.1]-, [2.1.1]-, [2.2.1]-, and [2.2.2]propellanes.

Geometry. The calculated optimized geometries are presented in Table 2. In the absence of any experimentally determined structural data of **1**, **2**, **3**, and **4** to assess the validity of the AM1 parametrization we give here for the purpose of comparison also the fully AM1 optimized tetrahedral geometry of adamantane with r_{CC} = 1.526 Å, $r_{CH_{methylene}}$ = 1.120 Å, and $r_{CH_{methine}}$ = 1.122 Å (experimental values are r_{CC} = 1.540 Å, $r_{CH_{methylene}} = r_{CH_{methine}}$ = 1.093 Å)[18] and of [1.1.1]propellane with r_{CC} = 1.547 Å, $r_{(CC)_{inv}}$ = 1.624 Å, $r_{CH_{methylene}}$ = 1.103 Å

(experimental values are $r_{CC} = 1.525$ Å, $r_{(CC)_{inv}} = 1.596$ Å, $r_{CH_{methylene}} = 1.106$ Å).[7e] The calculated C−C bond length for adamantane is shorter than the experimental (X-ray diffraction of orientationally disordered phase), while for the strained propellane they are longer (electron diffraction). Since the distance in bicyclo[1.1.1]pentane corresponding to $r_{(CC)_{inv}}$ in [1.1.1]propellane is calculated by AM1 at 1.875 Å, AM1 results are expected to be qualitatively correct especially in predicting trends within a group of molecules. The changes in structure on going from adamantane to molecules **1**, **2**, **3**, and **4** are significant. The relative degree of geometric strain in these molecules can be defined in terms of departure of C−C−C bond angles from the tetrahedral value. The bonds and angles deviate from the normal tetrahedral arrangement especially at the bridgehead carbons (C_2 and C_4 in Figure 1). The most significant changes concern the decreasing of the $C_2C_5C_4$ angle from 109.9° to 61.9° in **1**, 59.4° in **2**, 85.5° in **3**, and 85.0° in **4**. Thus, it is obvious that the bridgehead carbon atoms C_2 and C_4 have a great amount of geomeric strain. Concerning the C−C bond length variation, it is evident (Table 2) that the lengthening of C−C bonds is at most 2.7%, and shortening 2.0%. The most interesting aspect of the structure is the distance at the bridgehead region. The distance between bridgehead carbons in **1** is 1.567 Å and is in the range of measured values for a series of propellanes. The bond length is significantly shorter than the corresponding nonbonded distance of 2.130 Å in **3**. The analogous bridgehead−bridgehead distance in **2** is calculated to be 1.547 Å. In the case of its dihydro congener **4** the C_2-C_4 distance is 2.117 Å. For comparison, the calculated C_2-C_4 distance in adamantane is 2.490 Å and 1.624 Å in [1.1.1]-propellane. The calculations suggest that the central bond lengths in molecules **1** and **2** are close to the normal single C−C bond values of 1.540−1.560 Å. This is in agreement with the experimental data for other propellanes: 1.596 Å in [1.1.1]-propellane,[7e] 1.586 Å in some [1.1.1]propellane derivatives,[7f] 1.574 Å in aza[3.1.1]propellane derivative.[7d]

Internal Coordinates and Force Fields. The internal coordinates are the local group coordinates, defined in Table 3 and Figure 10. They have been selected according to the recommendations of Pulay et al.[18] These coordinates should make easier the comparison of the force constants between related molecules **1**, **2**, **3**, **4**, and adamantane. The number of internal coordinates for each molecule is specified in Table 4 (Supporting Information). Although it is possible to describe **1** and **2** without the central bond by using only the valence angles E_i, because of the numerous experimental facts (chemical activity, reactivity toward electrophiles and free radicals) and theoretical reasons (AM1 charge distribution, bond order, HOMO), we have decided not to omit the bridgehead bond as a separate internal coordinate. The internal coordinates related to CH and CH_2 groups and CCC deformations are identical to those used in the vibrational assignment of adamantane.[16] The other internal coordinates are related to the substituents. For deformation coordinates around a C_3 atom in species **2** and **4** the similarity with the CH_2 group is utilized and the internal coordinates are defined in terms of CC_2 scissoring, rocking, wagging, and twisting motions. The internal coordinates for CH_3 groups were constructed considering the local C_{3v} symmetry. The local symmetry coordinates of a given type have structure $A_1 + E$. For the doubly degenerate species E the internal coordinates are antisymmetrical CH_3 deformation and CH_3 rocking. In the construction of the molecular symmetry coordinates the overall C_s symmetry of molecules was utilized.

The AM1 method was used to obtain the force fields. The calculated force constants in Cartesian coordinates were transformed into those corresponding to the internal coordinates by using the generalized inverse of the **B** matrix.[16] They were then scaled with nine different scaling factors taken over from

TABLE 3: Local Group Internal Coordinates

internal coordinate[a]	description
R_i	CC stretching
K_i	methine CH stretching
L_i	methylene CH stretching
H_i	methyl CH stretching
$\Sigma_i \equiv (1/\sqrt{26})(5\gamma + \Omega)_i$	CH_2 scissoring
$P_i \equiv (1/2)(\beta_2 - \beta_1 + \beta_4 - \beta_3)_i$	CH_2 rocking
$\Psi_i \equiv (1/2)(-\beta_2 - \beta_1 + \beta_4 + \beta_3)_i$	CH_2 wagging
$T_i \equiv (1/2)(\beta_2 - \beta_1 - \beta_4 + \beta_3)_i$	CH_2 twisting
$A_i \equiv \alpha_i$	CH bending
$\Gamma_i \equiv (1/\sqrt{18})(4\delta_1 + \delta_2 + \delta_3)_i$	CCC deformation
$\Gamma_i'' \equiv (1/\sqrt{18})(4\delta_2 + \delta_1 + \delta_3)_i$	CCC deformation
$\Gamma_i'' \equiv (1/\sqrt{18})(4\delta_3 + \delta_2 + \delta_1)_i$	CCC deformation
$E_i \equiv \epsilon_i$	$(CCC)_\epsilon$ deformation[b]
$\Theta_i \equiv (1/\sqrt{26})(5\vartheta_1 + \vartheta_6)_i$	CC_2 scissoring
$X_i \equiv (1/2)(\vartheta_4 - \vartheta_2 + \vartheta_5 - \vartheta_3)_i$	CC_2 rocking
$\Phi_i \equiv (1/2)(-\vartheta_4 - \vartheta_2 + \vartheta_5 + \vartheta_3)_i$	CC_2 wagging
$\Omega_i \equiv (1/2)(\vartheta_4 - \vartheta_2 - \vartheta_5 + \vartheta_3)_i$	CC_2 twisting
$\Delta_i' \equiv (1/\sqrt{6})(\varphi_1 + \varphi_2 + \varphi_3 - \zeta_1 - \zeta_2 - \zeta_3)_i$	symmetrical CH_3 deformation
$\Delta_i'' \equiv (1/\sqrt{6})(2\varphi_1 - \varphi_2 - \varphi_3)_i$	antisymmetrical CH_3 deformation
$\Delta_i'' \equiv (1/\sqrt{2})(\varphi_2 - \varphi_3)_i$	antisymmetrical CH_3 deformation
$\Lambda_i' \equiv (1/\sqrt{6})(2\zeta_1 - \zeta_2 - \zeta_3)_i$	CH_3 rocking
$\Lambda_i'' \equiv (1/\sqrt{2})(\zeta_2 - \zeta_3)_i$	CH_3 rocking
$Z_i \equiv (1/\sqrt{3})(z_1 + z_2 + z_3)_i$	CH_3 torsion

[a] The definition of internal coordinate symbols is in connection with Figure 10. Local redundancies are connected with the CH methine groups, while the others are cyclic. With regard to molecular symmetry C_s they are distributed as 6 A′ + 4 A ″ in **1** and **2**, 6 A′ + 5 A″ in **3** and **4**. A similar situation is, of course, encountered in [1.1.1]propellane. Using the internal coordinates from ref 8a, one would expect, after eliminating the local methylene redundancies, 5 A_1', 2 A_2', 6 E′, A_1'', 3 A_2'', and 4 E″ modes. There are four redundancies left, and these are distributed as $A_1' + A_2'' + E''$. Of particular interest is that of A_1' symmetry because it involves the central bond: $\sum\Delta\epsilon_i = 0.5365 + \sum\Delta R_i - 3.0662\Delta R_7$, where ΔR_7 is the central bond stretching. The conclusion is that the vibrations of [1.1.1]propellane or any other propellane can be correctly described and assigned without taking into consideration the central C−C bond. The elimination has to be performed by an orthogonal transformation. [b] the notation $(CCC)_\epsilon$ denotes the outer bridgehead angle, $\angle C_1C_2C_5$, $\angle C_1C_2C_3$, etc.

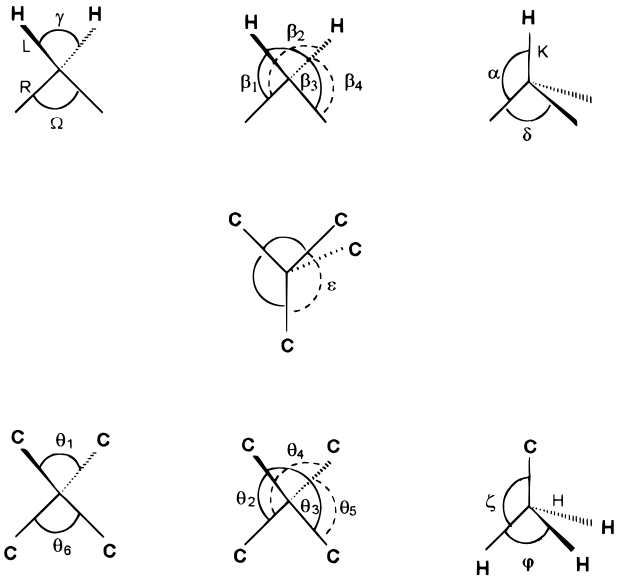

Figure 10. Labeling of angles in connection with the definitions of internal coordinates as given in Table 3.

adamantane and used for normal coordinate analysis. Vibrational assignment for adamantane[16] and its four isotopomers (adamantane-*1*-d_1, -*2*-d_1, -*2*,*2*-d_2, and -d_{16}) was obtained using not only high molecular symmetry, isotopic frequency shifts, and characteristic group frequencies but also empirical valence force field for alkanes. The scaling factors were calculated by the least-squares procedure to reproduce the isotopic frequency shifts as well. The assignments for **1**, **2**, **3**, and **4** proposed below are based on the assumed transferability of scaling factors (as the transferability of empirical force constants, it has a strong support in experimental findings). Similarity of the length and bond order of the central bond to those of an ordinary C−C bond justified the use of the same scaling factor. The value of the scaling factor for the CH stretching diagonal force constants was 0.910, and that of the CC stretching, 0.664. The scaling factors for diagonal force constants concerning CH_2 and CC_2 groups were set equal: for scissoring 1.059, for rocking 0.977, for wagging 0.967, and for twisting 1.157. For the diagonal force constants connected with CH bending the value of the scaling factor was 1.018. Equal scaling factors of 0.881 were assumed for the CCC deformations and for CH_3 symmetric and asymmetric deformations. CH_3 rocking force constants were scaled by the same scaling factor applied for scaling CH_2 and CC_2 rocking interactions. To account for the bridgehead region characteristic of propellanes and, on the other side, to keep the number of scaling factors as small as possible, only one additional scaling factor for $(CCC)_\epsilon$ deformations had to be introduced. Its value of 0.610 was obtained assuming that the strong IR bands of **1** and **2** at 580 and 590 cm^{-1}, respectively, are precisely the IR bands characteristic of all propellanes based on bridged bicyclobutanes.[6a−d] A scaling factor of 1.000 for the CH_3 torsion force constants was utilized. The off-diagonal force constants were scaled by the geometric mean value $(c_ic_j)^{1/2}$ except that the scaling factor of 0.232 for independent scaling of the off-diagonal force constants connected with all possible CC/CC stretching interactions was introduced (the same factor was used for adamantane to scale only interaction force constants between C−C bonds having a common C atom).

When the same scaling scheme was applied to [1.1.1]-propellane, the best factor values for CH_2 motions were close to the adamantane values, while those for the CC stretching and CC/CC stretching interactions were not. Besides, the calculated frequency of the ν_4 mode (central bond stretching) was 85 cm^{-1} too low. This could be improved only by introducing two additional factors, one for the central bond and another for the $CC/(CCC)_\epsilon$ interactions. Since the degree of structural similarity between adamantane and propellanes **1** and **2** can be considered much higher than between **1** or **2** and [1.1.1]-propellane, which is not a cagelike molecule, the transferability of the adamantane scaling factors has been assumed.

The choice of internal coordinates permitted a detail comparison of the force constants among compounds **1**, **2**, **3**, **4**, adamantane, and [1.1.1]propellane. The diagonal force constants for the CH stretchings are approximately the same. There is no significant differences between the force constants describing CH_2 group motions except for molecule **1**. The consequences of the different geometry for the CH_2 group on atom C_3 in **1** were the changed values of diagonal force constants. They were for rocking 49% smaller, for wagging 55% greater, and for twisting 29% greater in comparison with adamantane. The results for CH bending show a decrease of about 40% in the HC_5C_6 bending force constants in molecules **1** and **2**, about 22% in **3**, and 12% in **4**. Substitution has a quite appreciable effect on the molecular geometry of **1**, **2**, **3**, and **4**. A small increase in calculated C−C bond lengths and great changes in CCC angles in relation to adamantane are notable (Table 2). The departure from tetrahedral arrangement led to a geometric strain in all of these molecules. The most prominent changes relative to the admantane are the large coupling coefficients between force constants describing CC stretching vibrations having no common C atoms (these interaction force constants in adamantane are negligible). The most important CC stretching force constants are presented in Table 5. There is a general trend of diagonal CC stretching force constants toward smaller values (when compared to 4.296 aJ $Å^{-2}$ of adamantane) as a consequence of C−C bond lengthening. There are no great differences in CC stretching force constants among **1**, **2**, **3**, and **4**, except those connected to the substituent. For example, the substitution causes a 2.7% longer C_2-C_5 bond and 49% smaller C_2C_5 stretching force constants in all molecules. It should be added that the calculated CCC deformation force constants are significantly smaller than those for adamantane. The unusually small force constants for CCC deformations at the C_5 atom in all molecules are associated with the decreased $C_2C_5C_4$ angle values (about 46% smaller force constants).

TABLE 5: Part of the Scaled AM1 Force Field; CC Stretching Force Constants

	force constants[a]			
force constants[a]	**1**	**2**	**3**	**4**
C_1C_2	3.325	3.290	3.168	3.117
C_2C_5	2.067	2.034	2.185	2.183
C_5C_6	4.618	4.600	4.682	4.636
C_6C_7	3.400	3.470	3.973	4.074
C_7C_{11}	3.771	3.751	4.104	4.066
C_1C_{11}	4.277	4.258	4.389	4.346
C_1C_{10}	3.498	3.537	4.019	4.148
C_2C_3	2.808	2.587	2.759	2.499
C_3C_{12}		4.576		4.501
$C_2C_4 \equiv (CC)_{inv}$	1.071	1.282		
C_2C_5/C_4C_5	0.256	0.261	0.207	0.214
C_2C_5/C_5C_6	0.108	0.102	0.098	0.092
C_2C_5/C_6C_7	0.148	0.145	0.100	0.094
C_2C_5/C_7C_8	0.009	0.011	0.011	0.015
C_2C_5/C_7C_{11}	0.118	0.116	0.113	0.113
C_2C_5/C_1C_{11}	−0.007	−0.005	0.002	0.002
C_2C_5/C_8C_9	0.014	0.015	0.013	0.014
C_2C_5/C_9C_{10}	0.024	0.021	0.108	0.102
C_2C_5/C_1C_{10}	0.026	0.032	0.026	0.021
C_1C_2/C_2C_5	−0.091	−0.078	−0.075	−0.059
C_1C_2/C_4C_5	−0.004	−0.007	0.066	0.073
C_2C_5/C_2C_3	−0.115	−0.086	0.043	0.058
C_2C_3/C_4C_5	0.203	0.189	0.247	0.234
C_2C_5/C_3C_{13}		−0.008		−0.006
C_2C_5/C_3C_{12}		−0.003		−0.009
C_5C_6/C_6C_7	0.102	0.103	0.100	0.099
C_2C_3/C_3C_4	0.416	0.420	0.252	0.263
C_1C_2/C_6C_7	0.174	0.171	0.105	0.101
C_1C_2/C_7C_{11}	0.153	0.160	0.119	0.127
C_1C_2/C_9C_{10}	0.189	0.178	0.157	0.137

[a] Force constants are compatible with the energy measured in attojoules, bond lengths in angstroms, and angles in radians.

Relatively small values for the C_2-C_4 stretching force constants of 1.071 aJ $Å^{-2}$ in **1** and 1.282 aJ $Å^{-2}$ in **2** were obtained. They are the consequences of the atom distances (1.547 Å in **1** and 1.567 Å in **3**) and the choice of internal coordinates. The description of C_2 and C_4 atom motions through C_2C_4 stretching and six $(CCC)_\epsilon$ angles around bridgehead atoms (Table 5) reflects itself in the C_2C_4 stretching force constant values. A different set of internal coordinates without $(CCC)_\epsilon$ angles would give a significantly larger value of the C_2C_4 stretching force constant.[8a]

The remarkably different force constants couple the stretchings of the C−C bonds sharing a C atom relative to those with

no common C atom. The most interesting feature (Table 5) is the similarity between molecules **1** and **2**, as well as between **3** and **4**. The interaction force constants in molecule **1** have values comparable with the corresponding force constants in molecule **2**. The same conclusion can be deduced for molecules **3** and **4**. The inverted geometry of C_2 and C_4 atoms in species **1** and **2** has led to significant changes in values and even the signs of particular interaction force constants. For example, in the case of the C_1C_2/C_4C_5 interaction the force constant is 0.066 aJ Å^{-2} in **3** and 0.073 aJ Å^{-2} in **4**, while the small negative values of −0.004 aJ Å^{-2} in **1** and −0.007 aJ Å^{-2} in **2** were calculated. The comparison between coupling constants of C_2C_5/C_2C_3 stretching shows the same behavior: −0.115 aJ Å^{-2} in **1** and −0.088 aJ Å^{-2} in **2**, 0.043 aJ Å^{-2} in **3** and 0.058 aJ Å^{-2} in **4**. Thus the most important influence on the force field has the change from tetrahedral to inverted geometry, while the nature of substituents has minor influence especially on the part describing CCC skeleton motions.

Vibrational Analysis. Assuming the C_s symmetry for all compounds, all vibrations are both Raman and IR active. The molecule **1**, $C_{11}H_{14}$, has 69 normal modes, of which 40 are of A′ symmetry and 29 of A″. The 31 atoms in compound **2**, $C_{13}H_{18}$, give rise to 87 normal modes, 50 of which belong to class A′ and 37 to class A″. The molecule **3**, $C_{11}H_{16}$, has 27 atoms, which give rise to 75 internal normal vibrational modes. The normal modes are distributed among the symmetry species according to 43 A′ + 32 A″. The normal vibrations of compound **4**, $C_{13}H_{20}$, span the representation of 53 A′ and 40 A″.

The assignments of the vibrational spectra are based on the results of the scaled AM1 force fields, comparison with adamantane[16] and characteristic group frequencies, and the expectation that A′ modes should give rise to strong Raman and weak IR bands. In molecules **1** and **3** there should be at least 11 and in molecules **2** and **4** 13 normal modes being practically IR inactive. Any of these normal modes involves only those internal coordinates that are transformed into themselves by mirror reflection. The characteristic group modes arise from vibrations of the functional group in the molecule, the frequencies of which are only slightly affected by the molecular framework to which the group is bonded. The purpose was to find specific vibrational modes particularly sensitive to the nature of the substituent. Frequencies for the noncharacteristic fundamentals were then selected from the remaining unassigned bands in the spectrum. In this way was it possible to isolate the vibrational modes more connected with specific molecular structure, especially with the C_2-C_4 bond between inverted atoms.

Vibrational Assignment for Molecules 1 and 3. The similarity of the frequencies arising from CH and CH_2 groups to those of adamantane is quite striking. These vibrations are simply indicated in Tables 6 and 8 and will not be discussed further. According to the potential energy distribution (PED), it was possible to isolate the vibrations of the CH_2 group at the C_3 atom. The CH_2 stretchings are assigned to 3052 and 2938 cm^{-1} in **1** and **3**, respectively (Figure 4a). The frequencies of the CH_2 scissoring normal modes were found at 1499 cm^{-1} (**1**) and 1488 cm^{-1} (**3**) (Figure 4b). The calculations suggest that the CH_2 rocking mode in **1** is partially present at 1097 and 1052 cm^{-1}. The CH_2 rocking mode in molecule **3** is assigned to the band at 1085 cm^{-1}. In the A′ class of symmetry the CH_2 wagging normal modes are identified at 1135 cm^{-1} in **1** and at 1228 cm^{-1} in **3**. There exists a significant difference between molecules **1** and **3** associated with the CC/CC stretching interaction force constants, especially between those having no common C atom. The description of the CC stretching and CCC deformation vibrational modes according to the PED reflects different vibrational dynamics of molecules **1** and **3** and points toward the existence of a bond between inverted C atoms. The normal modes with the contributions of C_2C_3 and C_3C_4 stretching motions in **3** are observed at 942, 870, and 846 cm^{-1}. The corresponding normal modes in **1** were according to the normal coordinate analysis attributed to higher frequencies at 1145, 1097, and 1071 cm^{-1}. The most direct way to obtain the position of the stretching between inverted C_2 and C_4 atoms was the comparison of **1** and **3** spectra. The medium intense band in Raman spectra at 739 cm^{-1} and the strong Raman band at 672 cm^{-1} represent C_2C_4 stretching vibrations mixed with CCC deformations, because they are missing in the spectrum of **3** and also because all surrounding bands can be consistently explained (they have unchanged character compared to compound **3**) (Figure 5a). Both bands were found to be much weaker in IR spectra than in the Raman spectra. Since the Raman intensity is proportional to the square of the polarizability tensor derivative over the normal coordinate, this might be a consequence of the fact that the characteristic charge distribution in the bridgehead region contributes to the change of the polarizability.[8b] The experimental spectroscopic assignment of C_2C_4 stretching vibration frequencies is supported by the normal coordinate calculation. The two normal modes calculated at 743 and 672 cm^{-1} are described in terms of PED as the C_2C_4 stretching modes coupled with CC stretching and CCC deformation. The description of the strong IR 580 cm^{-1} band in **1** as an antisymmetric stretching of the outer C−C bonds coupled with $(CCC)_\epsilon$ deformations was actually assumed in order to achieve consistency with other small-ring propellanes.[6a−d]

Vibrational Assignment for Molecules 2 and 4. The observed Raman and IR bands for molecules **2** and **4** are compared with the calculated ones in Tables 7 and 9 (Supporting Information). To facilitate the approach, the characteristic fundamentals of methyl groups were first separated from other observed bands in the spectra. There are three methyl stretching modes around 3000 cm^{-1} and deformation modes around 1450 cm^{-1}, which are sensitive to the molecular framework to which the group is bonded. The stretching normal modes were observed at 3027 and 2919 cm^{-1} in Raman spectra of molecule **2** and at 3045 cm^{-1} in the Raman spectra of **4** (Figure 6a). The low symmetry of the surrounding of methyl groups was responsible for the mixing of local symmetry coordinates such as CH_3 symmetric and antisymmetric deformations. A relatively pure CH_3 symmetric deformation in **2** was found at 1375 cm^{-1} measured in Raman spectra (Figure 6b). The weak IR bands of **4** at 1345 and 1315 cm^{-1} and the medium intense IR band at 1330 cm^{-1} were described as CH_3 symmetric deformations (Figure 8). The large mixing between CH_3 symmetric and antisymmetric vibrations for molecule **2** was observed at 1325 and 1400 cm^{-1} for **4**. The vibrations in **2** and **4** around 1350 cm^{-1} are mixed; that is, each normal mode partakes of the nature of the CH_3 deformation vibration. The mixing occurs in **4** with CH_2 wagging at 1364 cm^{-1}, and with CH_2 wagging and CC stretching at 1354 cm^{-1}. The analogous fundamentals of **2** in A′ species were found at 1369, 1350, and 1345 cm^{-1}. The very weak Raman band of **2** at 1293 cm^{-1} (and 1295 cm^{-1} in IR spectra) was assigned to CC stretching vibrations mixed with CH_3 antisymmetric deformation and CC_2 scissoring. The weak IR band observed at 1000 cm^{-1} in **4** and the very weak Raman band of **2** at 1123 cm^{-1} were assigned as pure CH_3 rocking modes. The normal modes in **2** described in terms of CH_3 rocking motions were found in the A′ class at 1115, 1015, and 1006 cm^{-1} in the A″ class. The contributions of CH_3 rocking

TABLE 6. Observed and Calculated Frequencies (cm^{-1}) for 2,4-Methano-2,4-didehydroadamantane (1)[a]

mode	calc	obs Raman	infrared	PED
A′ ν_1	3032	3052 w	3050 w	CH_2 stretch.
ν_2	2989			CH stretch.
ν_3	2983			CH_2 stretch.
ν_4	2978			CH_2 stretch.
ν_5	2957			CH stretch.
ν_6	2948			CH_2 stretch.
ν_7	2943	2933 s		CH_2 stretch.
ν_8	2914		2920 s, bd	CH_2 stretch.
ν_9	2899			CH stretch.
ν_{10}	2883			CH_2 stretch.
ν_{11}	1503	1499 w	1500 vw	CH_2 sciss.
ν_{12}	1476		1480 w	CH_2 sciss.
ν_{13}	1457	1447 m	1465 m	CH_2 sciss.
ν_{14}	1441	1440 m		CH_2 sciss.
ν_{15}	1384	1380 w	1380 w	CH bend., CH_2 wagg.
ν_{16}	1342		1340 m	CH_2 wagg., CH bend., CC stretch.
ν_{17}	1339		1335 m	CH_2 wagg., CH bend.
ν_{18}	1303	1316 w	1315 w	CH_2 twist., CH_2 wagg., CC stretch.
ν_{19}	1279	1272 w		CH bend., CC stretch., CH_2 wagg.
ν_{20}	1246	1248 w		CH bend., CC stretch., CH_2 wagg.
ν_{21}	1230			CH bend., CC stretch.
ν_{22}	1170	1190 vw		CH bend., CC stretch., CH_2 twist.
ν_{23}	1129	1145 m		CC stretch., CH bend.
ν_{24}	1088	1097 w		CC stretch., CH_2 rock.
ν_{25}	1064	1071 w	1060 w	CH_2 rock., CC stretch., CCC def.
ν_{26}	1047	1048 vw		CH_2 rock., CC stretch.
ν_{27}	994	992 vw	995 w	CCC def., CH_2 rock.
ν_{28}	980	976 m		CC stretch., CCC def.
ν_{29}	924	929 w	930 w	CH_2 rock., CCC def., CC stretch.
ν_{30}	870		885 w	CC stretch., CH_2 rock., CCC def.
ν_{31}	830	836 w	830 w	CC stretch.
ν_{32}	798	765 s	765 w	CC stretch.
ν_{33}	728	739 m	740 vw	$(CC)_{inv}$ stretch.,[c] CC stretch., CCC def.
ν_{34}	717	708 m		CC stretch., CCC def.
ν_{35}	663	672 s	675 vw	$(CC)_{inv}$ stretch., CC stretch., CCC def.
ν_{36}	554	570 w		CCC def., $(CCC)_\epsilon$ def.
ν_{37}	484	483 m	485 vw	CCC def., $(CCC)_\epsilon$ def.
ν_{38}	417	455 w		CCC def., $(CCC)_\epsilon$ def.
ν_{39}	338	340 vw	350 w	$(CCC)_\epsilon$ def., CCC def.
ν_{40}	315			CCC def.
A″ ν_{41}	2955			CH stretch.
ν_{42}	2948			CH_2 stretch.
ν_{43}	2882			CH_2 stretch.
ν_{44}	2876	2858 m	2860 s	CH_2 stretch.
ν_{45}	1455		1450 m	CH_2 sciss.
ν_{46}	1376			CC stretch., CH_2 wagg.
ν_{47}	1351	1356 w	1355 w	CH bend., CH_2 wagg.
ν_{48}	1303		1300 w	CH_2 wagg., CH bend.
ν_{49}	1280		1285 w	CH_2 twist., CH_2 wagg., CC stretch.
ν_{50}	1238	1240 w		CH_2 twist., CH_2 wagg., CC stretch.
ν_{51}	1220		1225 w	CH_2 twist., CH bend.
ν_{52}	1211	1216 w	1195 w	CH_2 twist., CH bend.
ν_{53}	1168		1170 vw	CH_2 twist., CH bend., CH_2 wagg.
ν_{54}	1157		1160 w	CH bend, CH_2 wagg., CH_2 twist.
ν_{55}	1141		1135 vw	CH_2 wagg.
ν_{56}	1099		1100 w	CH_2 rock., CH bend., CC stretch.
ν_{57}	1052	1060 vw	1070 m	CC stretch., CH_2 twist., CH bend.
ν_{58}	1022	1022 w	1025 vw	CH bend., CH_2 wagg., CC stretch.
ν_{59}	964	977 w	980 w	CH_2 twist., CC stretch., CH_2 wagg.
ν_{60}	954		965 vw	CCC def., CC stretch., CH_2 rock.
ν_{61}	898	903 w		CH_2 rock., CH_2 wagg., CC stretch.
ν_{62}	833		840 w, sh	CC stretch., CCC def.
ν_{63}	788	804 vw	810 w	CC stretch., $(CCC)_\epsilon$ def., CH_2 wagg., CCC def.
ν_{64}	667		640 vw	CC stretch., $(CCC)_\epsilon$ def.
ν_{65}	615		580 s	CC stretch., $(CCC)_\epsilon$ def.
ν_{66}	477		500 w	CCC def.
ν_{67}	417	420 w	425 w	CCC def.
ν_{68}	318			CCC def., $(CCC)_\epsilon$ def., CC stretch.
ν_{69}	274	289 vw		CCC def.

[a] Symbols used: v, very; s, strong; w, weak; m, medium; bd, broad. [b] Contributions to PED are listed if larger than 10% and in descending order. [c] $(CC)_{inv}$ is C_2-C_4 stretching.

vibrations in molecule **4** normal modes were found in A′ species at 1246, 1178, 1160, 1020, and 997 cm^{-1} and in A″ species at 1200 and 1040 cm^{-1}.

Further specific vibrations of molecules **2** and **4** are certainly the methyl torsions. The IR spectrum of molecule **4** contains a very weak band at 365 cm^{-1}, which can be assigned as a

TABLE 8: Observed and Calculated Frequencies (cm^{-1}) for 2,4-Methanoadamantane (3)

mode	calc	obsd Raman	infrared	PED
A′ ν_1	3020			CH_2 stretch.
ν_2	3007	2998 w		CH stretch.
ν_3	2961			CH_2 stretch.
ν_4	2946			CH_2 stretch.
ν_5	2944			CH_2 stretch.
ν_6	2941	2938 vw		CH_2 stretch.
ν_7	2925	2918 s		CH stretch.
ν_8	2913			CH stretch.
ν_9	2904			CH stretch.
ν_{10}	2882			CH_2 stretch.
ν_{11}	2879	2849 m		CH_2 stretch.
ν_{12}	1568			CH_2 sciss.
ν_{13}	1493	1488 vw	1490 vw	CH_2 sciss.
ν_{14}	1463	1463 vw	1460 m	CH_2 sciss.
ν_{15}	1447	1438 w	1440 w, sh	CH_2 sciss.
ν_{16}	1389			CH bend., CH_2 wagg.
ν_{17}	1350	1353 vw	1355 vw	CH_2 wagg., CH bend., CC stretch.
ν_{18}	1344	1343 vw		CH_2 wagg., CH bend., CH_2 twist.
ν_{19}	1337		1325 vw	CH_2 wagg., CH_2 twist., CH bend.
ν_{20}	1301		1305 vw	CH bend., CH_2 wagg.
ν_{21}	1277	1288 vw		CH bend., CC stretch., CH_2 wagg.
ν_{22}	1255			CH bend., CH_2 twist.
ν_{23}	1209	1212 vw	1210 vw	CH bend., CH_2 wagg.
ν_{24}	1168	1184 m		CH bend., CC stretch.
ν_{25}	1139	1139 vw	1135 vw	CC stretch., CH bend.
ν_{26}	1101	1099 w	1100 w	CH_2 rock., CC stretch., CCC def.
ν_{27}	1083		1085 vw	CH_2 rock., CCC def., CC stretch.
ν_{28}	1055	1057 w	1058 w	CH_2 rock., CCC def., CC stretch.
ν_{29}	1004	995 m	990 vw	CH_2 rock., CCC def.
ν_{30}	968			CC stretch., CCC def.
ν_{31}	952			CC stretch., CH_2 rock., CCC def.
ν_{32}	945	942 m	945 w	CC stretch., CH_2 rock., CCC def.
ν_{33}	857	870 w		CC stretch., CCC def.
ν_{34}	832	845 w	845 vw	CC stretch., CCC def.
ν_{35}	801	800 vw	800 vw	CC stretch.
ν_{36}	770	764 s	760 vw	CC stretch.
ν_{37}	701	725 s	720 vw	CC stretch.
ν_{38}	656	647 w	660 vw	CCC def., CC stretch.
ν_{39}	575	573 m	580 vw	CCC def., CC stretch.
ν_{40}	531	505 w	510 vw	CCC def., CC stretch.
ν_{41}	482	472 w	480 vw	CCC def.
ν_{42}	406	398 vw	400 vw	CCC def.
ν_{43}	335	345 vw		CCC def.
A″ ν_{44}	3006		3000 m	CH stretch.
ν_{45}	2946		2970 m	CH_2 stretch.
ν_{46}	2912		2910 s, bd	CH stretch.
ν_{47}	2880			CH_2 stretch.
ν_{48}	2876		2860 s	CH_2 stretch.
ν_{49}	1458	1450 w, sh	1450 m	CH_2 sciss.
ν_{50}	1388	1374 vw	1375 vw	CH_2 wagg., CH bend., CC stretch.
ν_{51}	1354		1345 m	CH_2 wagg., CH bend.
ν_{52}	1319	1312 vw	1315 vw	CH_2 wagg., CH bend.
ν_{53}	1303		1305 vw	CH bend.
ν_{54}	1288		1280 vw	CH_2 twist., CC stretch.
ν_{55}	1269	1271 w	1265 w	CH_2 wagg., CH bend., CC stretch.
ν_{56}	1249			CH_2 twist., CC stretch.
ν_{57}	1231	1228 w	1230 w	CH_2 wagg., CH_2 twist., CH bend.
ν_{58}	1203			CH_2 wagg., CH_2 twist., CH bend.
ν_{59}	1179		1180 vw	CH bend., CH_2 twist., CH_2 wagg.
ν_{60}	1163	1156 w	1155 vw	CH bend., CH_2 wagg.
ν_{61}	1121	1110 m	1110 w	CH_2 twist., CC stretch., CH bend.
ν_{62}	1092			CH bend., CC stretch., CH_2 twist.
ν_{63}	1069	1070 w	1070 w	CC stretch., CH bend., CH_2 twist.
ν_{64}	1051	1044 w	1045 vw	CC stretch., CH_2 rock., CH bend.
ν_{65}	1000	1020 w	1020 vw	CH_2 twist., CC stretch., CH_2 rock.
ν_{66}	967			CH_2 rock., CC stretch.
ν_{67}	936	931 w	920 w	CH_2 rock., CC stretch.
ν_{68}	897	890 m	885 vw	CH_2 rock., CC stretch.
ν_{69}	802	820 w	815 w	CC stretch., CCC def.
ν_{70}	785		770 vw	CC stretch.
ν_{71}	635	623 vw	630 vw	CCC def., CC stretch.
ν_{72}	455	444 vw		CCC def.
ν_{73}	424	425 w		CCC def.
ν_{74}	325	330 vw		CCC def.
ν_{75}	271	286 w		CCC def.

CH_3 torsion. In the spectra of molecule **2** the normal mode connected to the pure CH_3 torsion motions is missing, and the very weak Raman band measured at 310 cm^{-1} was assigned as a combination vibration of CCC deformation and CH_3 torsion (Figure 7b). Here again the strong IR band of **2** at 590 cm^{-1} is the A″ normal mode in which stretchings of the outer C−C bonds are coupled not only with $(CCC)_6$ deformations but also with CC_2 waggings.

Vibrational Assignment of the Central C_2−C_4 Bond in Propellane 2. A comparative study of Raman spectra of propellane **2** and its dihydro counterpart **4** together with the monitoring of the chemical reaction of propellane **2** with DMDS has made it possible to establish the specific vibrations connected with the C_2−C_4 central bond. As in the previous case (molecules **1** and **3**), the inspection of the CC stretching region between 800 and 650 cm^{-1} in the spectra of **2** and **4** was of special interest. The band position in those regions of spectra is associated in large part with skeletal vibrations. Comparison of the spectra of the two molecules **2** and **4** reveals a significant difference in the CC stretching region (Figure 7a). According to the calculated PED, the stretching vibrations between inverted C_2 and C_4 atoms in compound **2** were attributed to the medium intense Raman band measured at 840 cm^{-1} and to the strong Raman band at 764 cm^{-1}. The normal mode calculated at 761 cm^{-1} is assigned as an almost pure C_2C_4 stretching vibration. It was evident that these bands were not found in any of the spectra of molecule **4**. The intensity of the band at 764 cm^{-1} measured in IR spectra of **2** is very low, as in the case of **1**. A comparison in terms of PED between the fundamentals of **1** and **3** has enabled the explanation of the influence of structural changes on the normal modes. The structural changes on the C_2 and C_4 atoms lead to significant changes in the character of normal modes. This is particularly valid for the C−C stretching vibrations. The Raman spectral region from 800 to 600 cm^{-1} contains the bands that reflect the best structural differences between propellanes and their congeners (Figure 5). The normal mode of **3** at 765 cm^{-1} can be interpreted as a CC stretching vibration connected with C_1, C_7, C_8, C_9, C_{10}, and C_{11}, i.e. with the cyclohexane ring that has no common atom with the bridgehead region. The vibrational band of **1** at 764 cm^{-1} has the same, unchanged character. The normal coordinate calculations attribute the strong 725 cm^{-1} band of **3** to the C_1C_2, C_4C_9, C_2C_5, C_4C_5, C_7C_8, and C_7C_{11} stretching vibrations. In the case of **1**, due to the changes from tetrahedral to the inverted geometry at the C_2 and C_4 atoms, three bands occur having partially the character of the 725 cm^{-1} mode of **3**. The band at 739 cm^{-1} belongs to the $(CC)_{inv}$, C_1C_2, and C_4C_9 stretching vibrations. The normal mode at 708 cm^{-1} is described as C_7C_8 and C_1C_2 stretching. The intense band found at 672 cm^{-1} is interpreted as C_1C_2 and C_4C_9 stretching mixed with the $(CC)_{inv}$ stretching vibration. The same approach applies to the vibrational analysis of **2** and **4**.

It has been pointed out that molecules **3** and **4** have a great number of modes having very similar PED. The character of some modes has been changed due to the mixing with the vibrations of the CH_3 groups. This is the reason for the appearance of bands at the new positions and with changed intensities. In the spectra of **4** the 764 and 725 cm^{-1} bands of **3** are missing. According to the calculations, the normal mode at 781 cm^{-1} of **4** has the same character as the normal mode at 765 cm^{-1} of **3**. The band at 737 cm^{-1} of **4** has unchanged character compared to the 725 cm^{-1} mode of **3**. None of the normal modes of **2** contain the same contribution from CC stretching vibrations as the 765 and 764 cm^{-1} modes observed in **1** and **3**. The normal mode observed at 764 cm^{-1} originates from the C_1C_2, C_4C_9, and $(CC)_{inv}$ stretchings, as does the mode at 672 cm^{-1} of **1**.

Conclusion

By combining the results of spectroscopic investigations and molecular orbital AM1 calculations, the central bond between inverted carbon atoms is associated with the HOMOs in [3.1.1]-propellanes **1** and **2**. The HOMOs of **1** and **2** are σ-type molecular orbitals. There is an increase in the electronegativity of C_2 and C_4 atoms in **1** and **2**, but electron density of the central bond is considerably higher at the back side of the inverted carbon atoms than between them. This is in good agreement with experimental results and the results of previous *ab initio* calculations.[4,8a] In the normal coordinate analysis of propellanes the use of the central bond stretching as an internal coordinate is not mandatory. However, by considering all the experimental facts and requiring the simplicity of the PED, it has been introduced into our description of the propellane vibrations.

The monitoring of the spectral changes of propellane **2** in reaction with DMDS (Figure 3) has revealed that the most remarkable observed feature was the disappearance of a strong band at 764 cm^{-1}. The assignment of this band as a normal mode connected to the C_2−C_4 stretching vibration is supported by the comparative spectroscopic study of **1** and **3**, and **2** and **4**. The qualitative explanation may be again given in terms of distribution of the negative charge concentrated within the C_2−C_4 region, which changes the polarizability of molecule **2** during Raman scattering.

Acknowledgment. We thank Dr. K. Furić for help in recording the Raman spectra. This work was supported by the Ministry of Science and Technology of the Republic of Croatia (Projects 1-03-066, 1-07-139, and 1-07-187) and in a part by the U.S.-Croatia Joint Fund No. JF 141 in cooperation with the National Science Foundation and the Ministry of Science and Technology.

Supporting Information Available: Table 4 of the numbers of internal coordinates according to the type for molecules **1**, **2**, **3**, and **4**: Table 7 and Table 9 of the observed and calculated frequencies for molecules **2** and **4**, respectively (12 pages). Ordering information is given on any current masthead page.

References and Notes

(1) (a) For reviews see: Ginsburg, D. *Propellanes: Structure and Reactions*; Verlag Chemie, GmbH: Weinheim, 1975. (b) Ginsburg, D. *Propellanes: Structure and Reactions*; Sequels I and II; Department of Chemistry, Technion: Haifa, 1980 and 1985. (c) Wiberg, K. B. *Acc. Chem. Res*. **1984**, *17*, 379. (d) Ginsburg, D. In *The Chemistry of the Cyclopropyl Group*; Rappoport, Z., Ed.; Wiley: Chichester, 1987; Chapter 19. (e) Wiberg, K. B. *Chem. Rev*. **1989**, *89*, 975.

(2) (a) Newton, M. D.; Schulman, J. M. *J. Am. Chem. Soc*. **1972**, *94*, 773. (b) Newton, M. D.; Schulman, J. M. *J. Am. Chem. Soc*. **1972**, *94*, 4391. (c) Stother, W.-D.; Hoffmann, R. *J. Am. Chem. Soc*. **1972**, *94*, 779. (d) Jackson, J. E.; Allen, L. C. *J. Am. Chem. Soc*. **1984**, *106*, 591. (e) Zilberg, S. P.; Ioffe, A. I.; Nefedov, O. M. *Izv. Akad. Nauk SSSR, Ser. Khim*. **1984**, 358. (f) Ushio, T.; Kato, T.; Ye, K.; Imamura, A. *Tetrahedron* **1989**, *45*, 7743.

(3) (a) Wiberg, K. B. *J. Am. Chem. Soc*. **1983**, *105*, 1227. (b) Wiberg, K. B.; Bader, R. F. W.; Lau, C. D. H. *J. Am. Chem. Soc*. **1987**, *109*, 985. (c) Wiberg, K. B.; Bader, R. F. W.; Lau, C. D. H. *J. Am. Chem. Soc*. **1987**, *109*, 1001.

(4) Feller, D.; Davidson, E. R. *J. Am. Chem. Soc*. **1987**, *109*, 4133.

(5) (a) Dodziuk, H. *Tetrahedron* **1988**, *44*, 2951. (b) Dodziuk, H. *J. Comput. Chem*. **1984**, *5*, 571.

(6) (a) Michl, J.; Radziszewski, G. J.; Downing, J.; Wiberg, K. B.; Walker, F. H.; Miller, R. D.; Kovačić, P.; Jawdosiuk, M.; Bonačić-Koutecky, V. *W. Pure. Appl. Chem*. **1983**, *55*, 315. (b) Pierini, A. B.; Reale, H. F.; Medrano, J. A. *J. Mol. Struct. (THEOCHEM)* **1986**, *148*, 109. (c) Walker, F. H.; Wiberg, K. B. *J. Am. Chem. Soc*. **1982**, *104*, 2056. (d) Wiberg, K. B.; Walker, F. H.; Pratt, W. E. *J. Am. Chem. Soc*. **1983**, *105*, 3638.

(7) (a) Wiberg, K. B.; Burgmaier, G. J.; Shen, K.; La Placa, S. J.; Hamilton, W. C.; Newton, M. D. *J. Am. Chem. Soc.* **1972**, *94*, 7402. (b) Szeimies-Seebach, U.; Harnisch, J.; Szeimies, G.; van Meersche, M.; Germain, G.; Declerq, J.-P. *Angew. Chem., Int. Ed. Engl.* **1978**, *17*, 848. (c) Szeimies-Seebach, U.; Szeimies, G.; Van Meerssche, M.; Germain, G.; Declerq, J.-P. *Nouv. J. Chim.* **1979**, *3*, 357. (d) Chakrabarti, P.; Seiler, P.; Dunitz, J. D.; Schülter, A.-D.; Szeimies, G. *J. Am. Chem. Soc.* **1981**, *103*, 7378. (e) Hedberg, L.; Hedberg, K. *J. Am. Chem. Soc.* **1985**, *107*, 7257. (f) Seiler, P.; Belzner, J.; Bunz, U.; Szeimies, G. *Helv. Chim. Acta* **1988**, *71*, 2100.

(8) (a) Wiberg, K. B.; Dailey, W. P.; Walker, F. H.; Waddell, S. T.; Crocker, L. S.; Newton, M. D. *J. Am. Chem. Soc.* **1985**, *107*, 7247. (b) Wiberg, K. B.; Waddell, S. T.; Rosenberg, R. E. *J. Am. Chem. Soc.* **1990**, *112*, 2184.

(9) (a) Honegger, E.; Huber, H.; Heilbronner, E.; Dailey, W. P.; Wiberg, K. B. *J. Am. Chem. Soc.* **1985**, *107*, 7172. (b) Eckert-Maksić, M.; Mlinarić-Majerski, K.; Majerski, Z. *J. Org. Chem.* **1987**, *52*, 2098. (c) Gleiter, R.; Pfeifer, K.-H.; Szeimies, G.; Belzner, J.; Lehne, K. *J. Org. Chem.* **1990**, *55*, 636.

(10) Mlinarić-Majerski, K.; Majerski, Z.; Rakvin, B.; Veksli, Z. *J. Org. Chem.* **1989**, *54*, 545.

(11) (a) Mlinarić-Majerski, K.; Majerski, Z. *J. Am. Chem. Soc.* **1980**, *102*, 1418. (b) Mlinarić-Majerski, K.; Majerski, Z. *J. Am. Chem. Soc.* **1983**, *105*, 7389.

(12) (a) Mlinarić-Majerski, K.; Šafar-Cvitaš, D.; Majerski, Z. *Tetrahedron Lett.* **1991**, *32*, 1655. (b) Mlinarić-Majerski, K.; Šafar-Cvitaš, D.; Veljković, J. *J. Org. Chem.* **1994**, *59*, 2374.

(13) Majerski, Z.; Mlinarić-Majerski, K. *J. Org. Chem.* **1986**, *52*, 3219.

(14) Lin-Vien, D.; Colthup, N. B.; Fately, W. G.; Grasselli, J. G. *The Handbook of Infrared and Raman Characteristic Frequencies of Organic Molecules*; Academic Press: New York, 1991; p 231.

(15) Stewart, J. J. P. *J. Comput.-Aided Mol. Des.* **1990**, *4*, 1.

(16) Bistričić, L.; Baranović, G.; Mlinarić-Majerski, K. *Spectrochim. Acta* **1995**, *51*, 1643, and references therein.

(17) Average value from (a) Mansson, M.; Rapport, N.; Westrum, E. F. *J. Am. Chem. Soc.* **1970**, *92*, 7296 and (b) Butler, R. S.; Carson, A. S.; Laye, P. G.; Steele, W. V. *J. Chem. Thermodyn.* **1971**, *3*, 277.

(18) Nordman, C. E.; Schmitkons, D. L. *Acta Crystallogr.* **1965**, *18*, 764.

(19) Pulay, P.; Fogarasi, G.; Pang, F.; Boggs, J. E. *J. Am. Chem. Soc.* **1979**, *101*, 2550.